electronics

Article

Effects of Material Deformation Due to Aging of Electrical Steel on the Brushless Wound-Field Synchronous Generator

Jae-Beom Kang [1,2], Ji-Young Lee [1,2,*], Tung Nguyen [1,2], Hyeong-Jin Kim [2] and Ji-Heon Lee [2,3]

[1] Energy and Power Conversion Engineering Department, Korea University of Science and Technology, Daejeon 34113, Republic of Korea; kangjb@keri.re.kr (J.-B.K.); tungnguyen@keri.re.kr (T.N.)
[2] Air Mobility Electric-Motor & Drive Research Team, Korea Electrotechnology Research Institute, Changwon 51543, Republic of Korea; khjin@keri.re.kr (H.-J.K.); ljh0524@keri.re.kr (J.-H.L.)
[3] Mechanical Engineering Department, Pusan National University, Busan 80401, Republic of Korea
* Correspondence: jylee@keri.re.kr

Abstract: This study analyzes the material deformation of electrical steel with aging and its effects on the electromagnetic and thermal characteristics of a Brushless Wound-Field Synchronous Generator (BL-WFSG). First, in order to confirm the material deformation of electrical steel applied to the BL-WFSG, magnetic property tests are performed on the core sheets of the old and new generators. Those two generators are made of the same material, so there was no difference except for their usage time. Based on the results of the magnetic property tests, an electromagnetic field analysis is performed on the old and new generators, and analysis results are compared in order to confirm the effects of material deformation on the electromagnetic characteristics of BL-WFSG. Then, a thermal analysis is performed on the old and new generators using losses calculated by electromagnetic field analysis as heat sources, and analysis results are compared in order to confirm the effects of material deformation on the thermal characteristics of BL-WFSG. Finally, an additional electromagnetic analysis is performed on both the old and new generators, using the exact winding resistances that were calculated in the thermal analysis for each respective generator in order to calculate and compare the efficiency of the old and new generators. Through this process, the authors confirmed the effects of material deformation of the rotor and stator cores due to aging on the electromagnetic and thermal characteristics of the BL-WFSG.

Keywords: wound field synchronous machine; material deformation; aging effect

Citation: Kang, J.-B.; Lee, J.-Y.; Nguyen, T.; Kim, H.-J.; Lee, J.-H. Effects of Material Deformation Due to Aging of Electrical Steel on the Brushless Wound-Field Synchronous Generator. *Electronics* **2023**, *12*, 2279. https://doi.org/10.3390/electronics12102279

Academic Editors: Junghwan Chang, Anindya Nag and Sarbajit Paul

Received: 25 April 2023
Revised: 12 May 2023
Accepted: 16 May 2023
Published: 18 May 2023

1. Introduction

A Brushless Wound-Field Synchronous Generator (BL-WFSG) consists of an automatic voltage regulator (AVR), an exciter, and a main generator, as shown in Figure 1 [1–3]. Unlike the slip ring and brush combination that requires physical contact, the combination of the AVR and exciter serves to supply direct current to the field winding of the main generator without physical contact, and the main generator receiving the field current converts mechanical input power to electrical output power [4–6]. In addition, the AVR and exciter combination of BL-WFSG is equipped with a system that automatically adjusts the magnitude of the field current to maintain the same output in the entire operating speed range. This system can cut off the supply of field current quickly when problems such as a short in the winding occur to prevent further failure. For this reason, BL-WFSG has been used in various systems such as military applications that require high durability and reliability because of the absence of maintenance burden caused by wear and tear of brushes and slip rings.

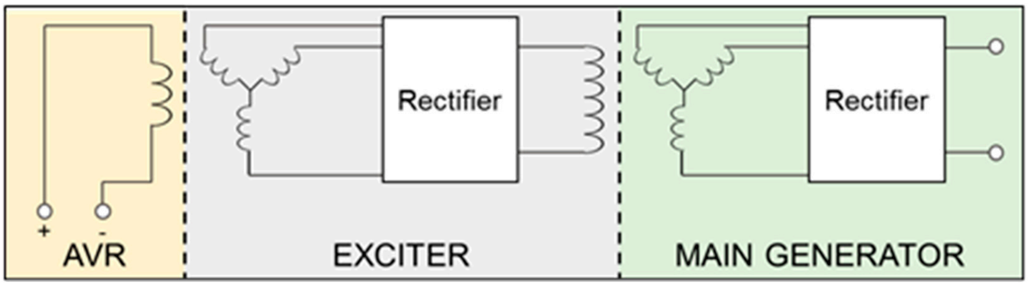

Figure 1. Equivalent circuit of Brushless Wound-Field Synchronous Generator.

The BL-WFSG studied in this paper has been applied to a specific application as an engine-generator. Therefore, the rotational speed of the BL-WFSG is dependent on the engine speed. As a result, the base speed of the BL-WFSG can be considered as 3500 RPM, which is the speed at which the engine is started, and the maximum speed of the BL-WFSG can be considered as 13,000 RPM, which is the maximum speed of the engine. However, as mentioned earlier, the output power of the BL-WFSG remains constant at all rotational speeds. This generator has been in operation for more than 30 years, but with the gradual aging of the generator, the magnitude of the field current for the same output power has increased. This problem may occur if the efficiency of the BL-WFSG gradually decreased due to aging. When the efficiency decreases, the output power decreases at the same input power, and the field current increases through the AVR and exciter combination system to compensate for this.

The factors that cause this decrease in the efficiency of the electric machine due to aging can be primarily attributed to two types of factors: dimensional deformation and material deformation [7–9].

Dimensional deformation refers to the changes in the dimensions of the core in electric machines due to heat or external stress. In particular, dimensional deformation of the stator and rotor parts around the air gap, where input power is converted to output power, can have a significant impact on the output characteristics of the electric machine. If the air gap length is changed, the output power can be decreased. It usually occurs when the electric machine has suffered fatigue stress for a long time [7]. Material deformation refers to the changes in the magnetic properties such as B-H curve and core loss of the rotor and stator cores. It can occur when electrical steel that consists of the electric machine has suffered corrosion or thermal deterioration [8,9]. In [7–9], the authors studied the dimensional or material deformation of electrical steel that is applied to the electric machine. However, they only focused on electrical steel, not the electric machine. Therefore, it is difficult to know the effects of the deformation of electric steel on the electric machine directly.

In this paper, the deformation of electrical steel due to aging, as well as the effect of such deformation on the electromagnetic and thermal characteristics of BL-WFSG are analyzed. In addition, the factors that increase the field current of BL-WFSG are also identified. Prior to analysis, the authors visually inspected the rotor and stator cores of the BL-WFSG that have been in operation for more than 30 years. It was confirmed that there was no dimensional deformation, but there was an increase in surface roughness of the cores. The increase in surface roughness of the core corresponds to material deformation rather than dimensional deformation. Therefore, this paper focuses on the material deformation of electrical steel sheets and its effects on the electromagnetic, thermal, and efficiency characteristics of the BL-WFSG.

2. Analysis Process for Material Deformation of Electrical Steel and Its Impact on BL-WFSG

Figure 2 demonstrates the analysis process for material deformation of electrical steel due to aging and its effects on the electromagnetic, thermal, and efficiency characteristics of the BL-WFSG. In the first step, in order to confirm the material deformation with the aging of electrical steel applied to the BL-WFSG, a magnetic property test is performed on the core sheet of an old generator (O-core) operated for ~30 years and the core sheet of a newly manufactured generator (N-core). The O-core and N-core were both made of 50PN510 (by POSCO) which is no-oriented electrical steel, and there were no differences except for their usage time. The magnetic properties of the O-core and N-core are compared in two cases. The first case is the B-H curve characteristic, and the second case is the core loss characteristic. Through this, material deformation of the core with aging is confirmed. In the second step, electromagnetic field analysis is performed on the new and old generator based on the magnetic property test results to analyze the effects of material deformation with aging of electrical steel on the electromagnetic characteristics of BL-WFSG. In the third step, in order to analyze the effects of material deformation with the aging of electrical steel on the thermal characteristics of BL-WFSG, thermal analysis is performed on the old and new generators using the losses calculated through electromagnetic field analysis as heat sources, and their thermal characteristics are compared and analyzed. Finally, in the fourth step, in order to analyze the effects of material deformation with aging of electrical steel on the efficiency characteristics of BL-WFSG, the efficiencies of the old and the new generators are calculated and compared based on the results of electromagnetic field analysis and thermal analysis.

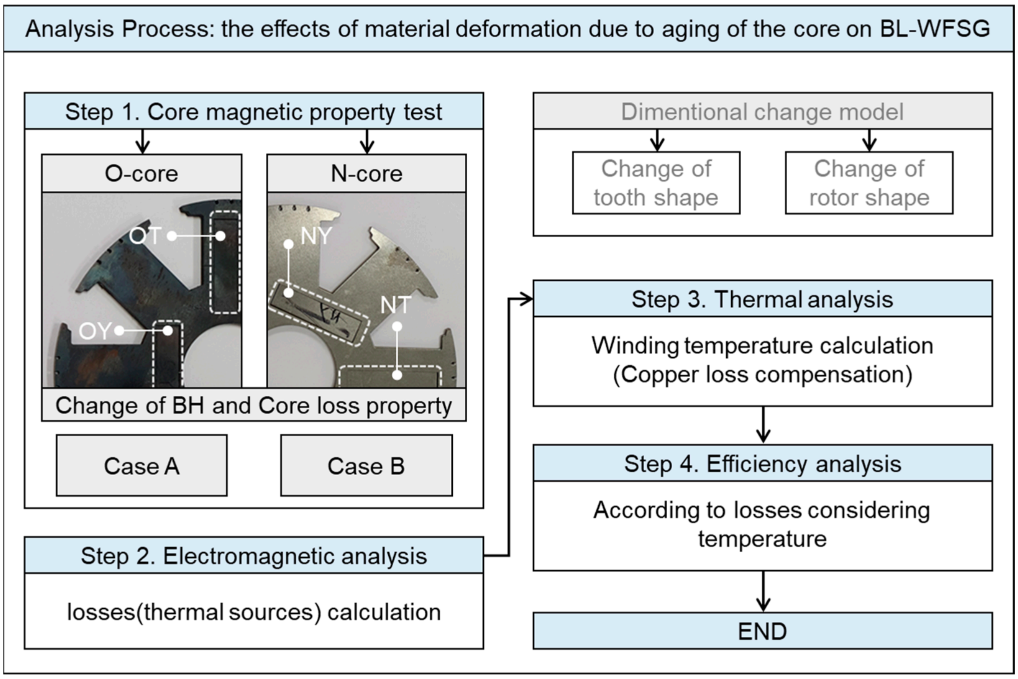

Figure 2. Analysis flowchart for material deformation of electrical steel with aging and its impact on BL-WFSG.

3. Core Magnetic Property Test

Magnetic property tests are conducted on samples extracted from the core sheets of new and old generators to analyze the changes in the B-H and core loss characteristics of the core due to the aging of BL-WFSG.

3.1. B-H Curve Measurement Test

In order to confirm the changes in the B-H curve with aging, the yoke part of the O-core and N-core was obtained, and the B-H curve test was performed. The B-H curve measuring device is MAGNET-PHYSIK's REMAGRAPH C-500, as shown in Figure 3a, and the specimens used for measuring the B-H curve are ring-shaped cores which are yoke parts of the core sheets as shown in Figure 3b. Those two specimens (O-core and N-core) were both made of 50PN510(by POSCO) which is non-oriented electrical steel, and there were no differences except for their usage time.

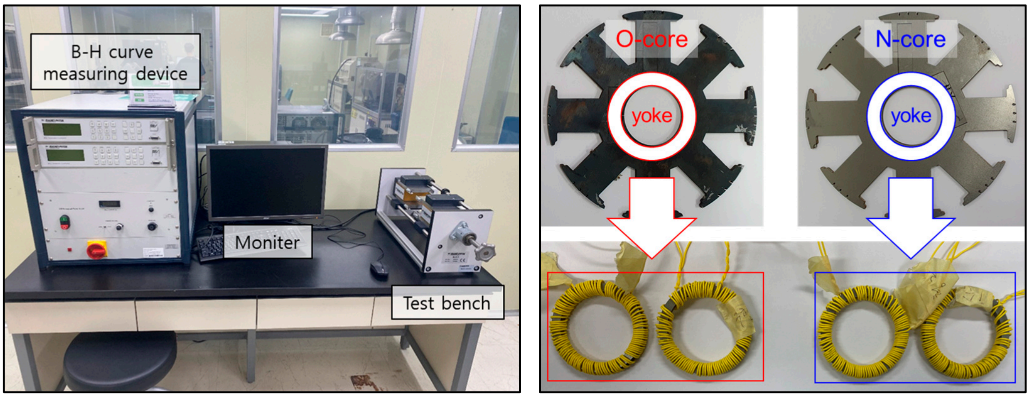

(**a**) (**b**)

Figure 3. (**a**) B-H curve measuring device; (**b**) specimens of O-core and N-core for B-H curve test.

The B-H curve measurement test results are shown in Figure 4, where it can be observed that the knee point of the O-core was higher than that of the N-core. This means that the O-core had a relatively high magnetic flux density compared to the N-core for the same coercive force. Therefore, it is assumed that the B-H characteristics of this generator have improved rather than deteriorated with aging.

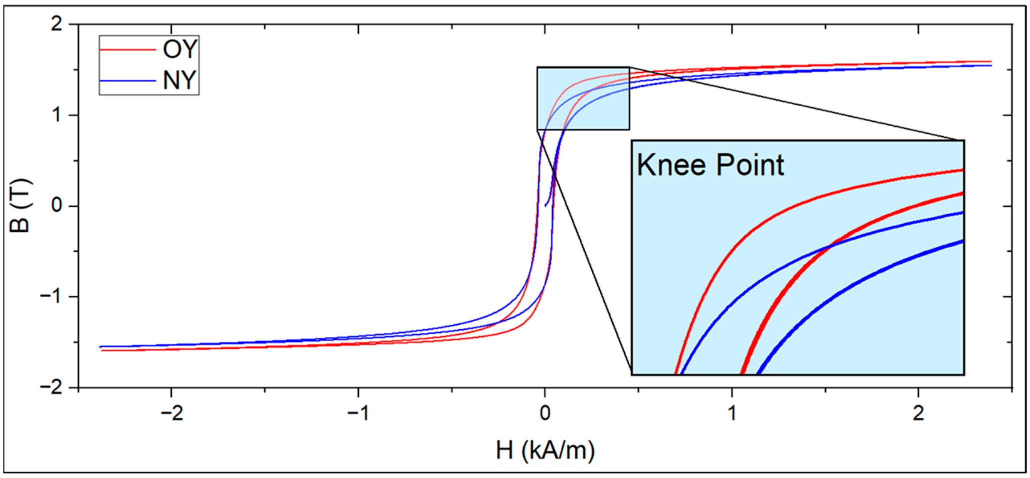

Figure 4. B-H curve test results for O-core and N-core.

3.2. Core Loss Measurement Test

In order to confirm the changes in the core loss with aging, the yoke and teeth parts of the O-core and N-core were obtained, and a core loss test was performed. The core loss measuring device is IWATSU's SY-956, as shown in Figure 5a, and the specimens used for measuring the core loss are bar-shaped cores which are yoke and teeth parts of the core sheets as shown in Figure 5b.

The core loss test results for each part are plotted in Figure 6. From Figure 6, it can be confirmed that a high core loss occurred in the O-core compared to that in the N-core for all frequency ranges. To further analyze the changes in core loss characteristics, bar graphs are presented in Figure 7, which presents the differences in core losses with respect to magnetic flux density at the base rotation frequency band of 200 Hz and the maximum rotation frequency band of 1000 Hz in the generator. At each frequency, the core loss in the yoke and tooth parts of each generator was averaged and compared to each other. It can be observed that at a relatively low flux density of 0.2 T, the O-core exhibits approximately 377% higher core losses at 200 Hz and 222% at 1000 Hz compared to the N-core. Similarly, at a relatively high flux density of 1.2 T, the O-core exhibits approximately 245% higher core loss at 200 Hz and 176% higher core loss at 1000 Hz compared to the N-core. From these results, it can be shown that the difference in core loss between the O-core and N-core decreases as the frequency increases. This is because at low frequencies, the change in magnetic flux density over time is slow, so the effect of changes in the magnetic properties of the core is more pronounced. However, at high frequencies, the change in magnetic flux density over time is fast, so the effect of changes in the magnetic properties of the core decreases.

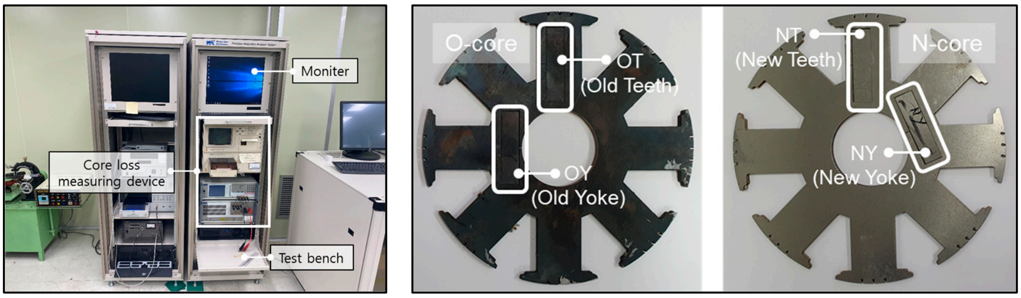

(**a**) (**b**)

Figure 5. (**a**) Core loss measuring device; (**b**) specimens of O-core and N-core for core loss test.

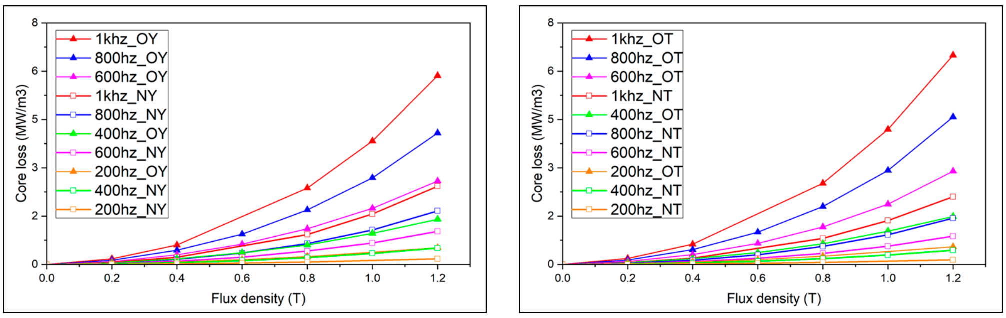

(**a**) (**b**)

Figure 6. Core loss test results for (**a**) yoke parts and (**b**) tooth parts for O-core and N-core.

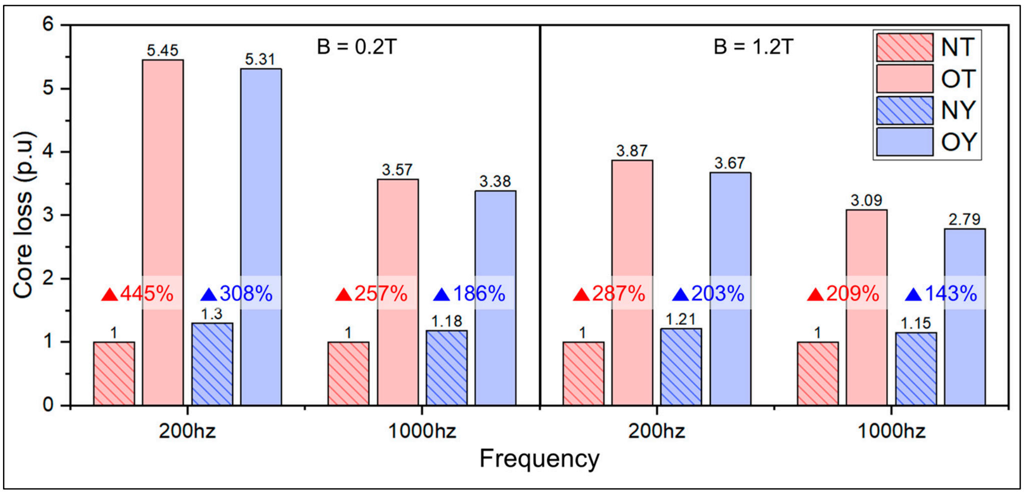

Figure 7. Core loss comparison bar graph.

3.3. Test Results Analysis

Through the magnetic property tests, it was confirmed that the core of the old generator, i.e., the O-core, showed relatively better B-H characteristics than the N-core, but had inferior core loss characteristics. In general, if the B-H characteristics of electrical steel are excellent, then its core loss characteristics are also excellent. However, in [10], the authors demonstrated through experiments that the B-H characteristics improved while the core loss characteristics decreased when tensile stress ranging from 0 to 7 MPa was applied to the electrical steel. Furthermore, in [11,12], the authors measured the B-H curve for electrical steel sheets subjected to tensile stress ranging from 0 to 73 MPa. As a result, it was observed that the B-H characteristics of non-oriented grain electrical steel sheets improved under tensile stress ranging from 0 to 20 MPa, but deteriorated under higher tensile stress. The BL-WFSG discussed in this paper operated at a high speed of up to 13,000 rpm. Therefore, a tensile stress was applied to the rotor. In addition, a thermal stress was applied to the stator and rotor as the operating temperature of the BL-WFSG was high. Because the old generator has been subjected to longer periods of tensile and thermal stress than the new generator, the B-H characteristics of the O-core may have been improved, but the core loss characteristics may have decreased. Due to these stresses, the B-H characteristics of the O-core may have been improved, but the core loss characteristics may have decreased.

Considering that the B-H characteristics slightly improved while the core loss characteristics decreased notably, it is assumed that the above-mentioned causes as well as other factors lowered the core loss characteristics. The factors for the deterioration of core loss characteristics of the core with aging include material degradation, corrosion, and physical deformation [7–9]. In fact, the inside of the BL-WFSG discussed in this paper contains oil to lower the temperature of the field and armature windings. Since the rotor and stator cores have been exposed to the oil for a long time, a combination of the above-mentioned factors may have resulted in an increased core loss. In this paper, the main focus is not on the material deformation of the core with aging, but rather on the effects of the material deformation on the electromagnetic, thermal, and efficiency characteristics of the BL-WFSG. Therefore, the causes of material deformation will not be further analyzed beyond this paragraph.

4. Electromagnetic Field Analysis

Electromagnetic field analysis is performed on the old and new generators based on the magnetic property test results to analyze the changes in the electromagnetic characteristics of BL-WFSG with aging. The BL-WFSG covered in this paper has a wide range of operating speeds. However, the BL-WFSG operates at 3500 RPM, which is the base speed of the generator, for more than 95% of the operating time, and at 13,000 RPM, which is the maximum speed of the generator, for less than 5% of the operating time. For this reason, the electromagnetic field analysis is performed on the old and new generators operating at 3500 RPM. The electromagnetic field analysis models of both generators have the same model of stator, rotor cores and winding as shown in Figure 8, and they reflect only the magnetic properties of the rotor and stator cores differently. That is, the magnetic characteristics of the O-core are reflected in the old generator, and the magnetic characteristics of the N-core are reflected in the new generator.

A 2D electromagnetic field finite element analysis was performed for both generators in steady state under the same load conditions using Ansys Electronics Desktop 2021 R2, and the results are listed in Table 1. The old generator had better B-H characteristics, but inferior core loss characteristics compared to the new generator, resulting in approximately 0.5% higher air-gap flux density, approximately 3.2% higher output power, and approximately 179% higher core loss.

In contrast to the difference in core losses, the differences in armature and field copper losses between the old and new generators were relatively small. This is because the winding temperature of both generators was assumed to be the same as the generator cooling oil, which was 120 °C. It is possible to confirm the winding temperature of both generators through thermal analysis, so the exact copper losses can be compared later.

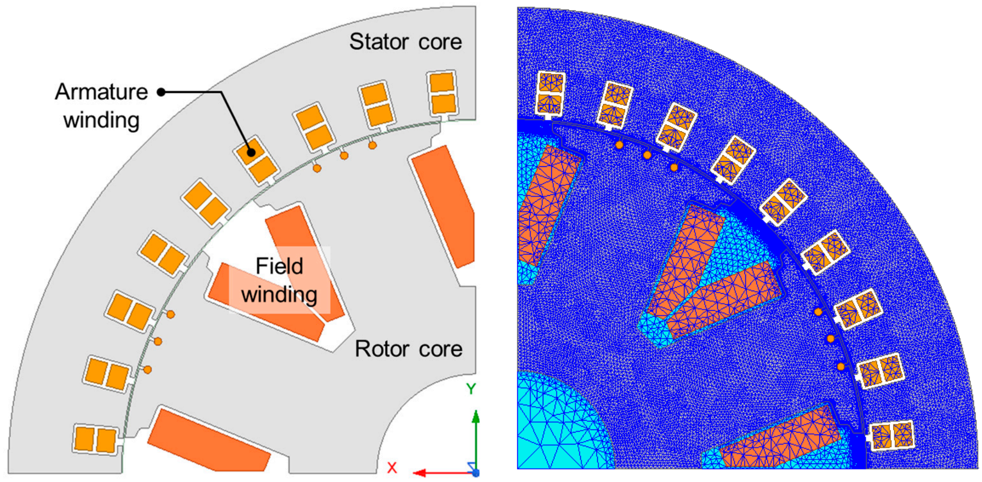

(**a**) (**b**)

Figure 8. (**a**) Electromagnetic field analysis model (1/4); (**b**) Meshed model (1/4).

Table 1. Electromagnetic field analysis results.

Parameter	New Generator	Old Generator	Difference
Rotational speed	3500 RPM		-
Field current	11 A		-
Average air-gap flux density	0.761 T	0.765 T	0.5%
Output power	16,760 W	17,304 W	3.2%
Core loss	422.3 W	1176 W	178%
Field copper loss	407.7 W		-
Armature copper loss	432 W	455.5 W	5.4%

Under the same load conditions, the old generator has a slightly higher output power than the new generator, but a much larger core loss. It was assumed to have relatively low efficiency. A detailed analysis was performed after calculating the exact copper loss through thermal analysis.

5. Thermal Analysis

In the electromagnetic field analysis, it was confirmed that the core loss of the old generator was much higher than that of the new generator. The core loss is the factor that increases the temperature of the generator and reduces efficiency. In order to analyze the effects of increased core loss on the thermal characteristics of the BL-WFSG, thermal analysis is performed on the old and new generators, and the analysis results are compared.

Thermal analysis methods include Computational Fluid Dynamics, Finite Element Analysis, and Lumped-Parameter Thermal Network (LPTN). In this study, thermal analysis is performed using LPTN, which has the advantage of shorter analysis time [13–15]. In order to perform the LPTN, the heat transfer coefficients considered the cooling conditions, and the heat sources are required. Since the external housing cooling and oil spray cooling were applied to the actual BL-WFSG, the heat transfer coefficients are calculated considering these two cooling methods by referring [13,16,17]. The losses calculated by electromagnetic field analysis—which are rotor core loss, stator core loss, armature winding copper loss, and field winding copper loss—are reflected as heat sources.

Based on the heat sources and heat transfer coefficients, the thermal equivalent circuits of both old and new generators were constructed, as shown in Figure 9, and steady-state thermal analysis was performed for each generator. Since the armature and field copper losses reflected in the thermal analysis were calculated assuming that the temperature of the winding was 120 °C, the analysis was repeated until the temperature of the winding and the copper loss that increased in proportion converged [18].

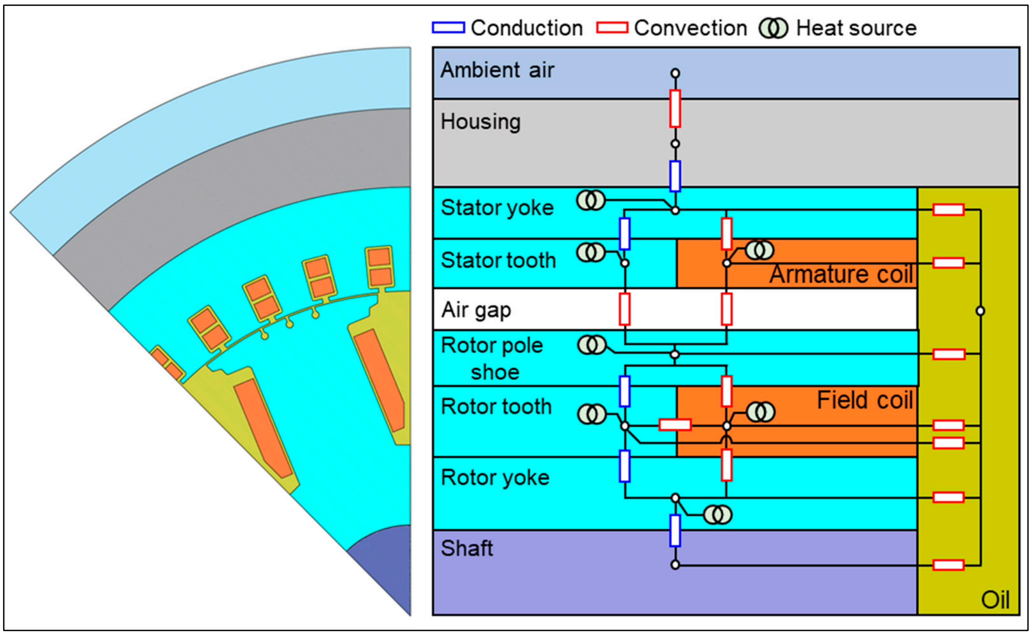

Figure 9. Thermal equivalent circuit.

Table 2 shows the thermal analysis of both generators operating at 3500 rpm. All components of the old generator showed higher temperatures than those of the new generator. In detail, the temperature differences between the old and new generator stator cores, rotor cores, armature winding, and field winding were about 11.4%, 8%, 4.5%, and 4%, respectively. Considering that the difference in heat losses for both generators was not high except for the core loss, it can be inferred that the main factor causing this temperature difference was the core loss. Furthermore, considering that the core loss increased proportionally with the square of the rotational frequency and that the operating speed range of the generator was 3500–13,000 rpm, it can be inferred that the temperature difference in the generators will increase even further with an increase in rotational speed.

Table 2. Thermal analysis results.

Parameter	New Generator	Old Generator	Difference
Stator core	125 °C	139.3 °C	11.4%
Rotor core	123 °C	132.8 °C	8.0%
Armature winding	121.8 °C	127.3 °C	4.5%
Field winding	144.8 °C	150.6 °C	4.0%

6. Efficiency Analysis

Through electromagnetic field and thermal analysis, it is possible to assume that the efficiency of the BL-WFSG has decreased with aging. In order to clearly confirm the efficiency of BL-WFSG decrease with aging, the efficiencies of both old and new generators are analyzed based on the exact temperatures of both the field and armature winding which were calculated by thermal analysis.

To calculate the winding resistance, the following equation can be used:

$$R_{ph} = \frac{T_{ph}}{a} \cdot \frac{L}{nA} \cdot \rho_0 [1 + \alpha (T - T_0)] \quad (1)$$

where R_{ph} is the winding resistance per phase, T_{ph} is the number of turns in series per phase, a is the number of parallel path, L is the mean turn length of the coil, n is the number of parallel strands in each conductor, A is the cross-sectional area of one strand, ρ_0 is the resistivity of copper at temperature of T_0, α is the temperature coefficient of the resistivity ratio, and T is the winding temperature.

The additional electromagnetic field analysis is performed on the old and new generators reflecting the calculated winding resistance by (1). In the additional electromagnetic field analysis, there are no differences in the load and input conditions except for the winding resistance.

Table 3 shows the additional electromagnetic field analysis results of the new and old generators operating at 3500 RPM. It was confirmed that the field copper losses of the old and new generators increased, and the difference between the two losses was about 2.1%, which is different from the initial electromagnetic analysis result as listed in Table 1. On the other hand, it was found that the armature copper losses of the old and new generators did not change significantly, and the difference between the two losses did not change much either. This is because the temperature of the armature windings of the old and new generators, calculated through thermal analysis, did not show significant differences compared to the assumed temperature in the initial electromagnetic field analysis. The output powers and core losses of both the old and new generators were found to be the same as the initial electromagnetic field analysis results.

Table 3. Additional electromagnetic field analysis results.

Parameter	New Generator	Old Generator	Difference
Input power	18,062 W	19,393 W	7.3%
Output power	16,760 W	17,304 W	3.2%
Efficiency	92.8%	89.2%	4.0%
Core loss	422 W	1176 W	178.5%
Field copper loss	448 W	457 W	2.1%
Armature copper loss	432 W	456 W	5.4%

The output power of the old generator was about 3.2% higher than that of the new generator, and the input power of the old generator was about 7.3% higher than that of the new generator. As a result, the efficiency of the old generator was about 4% lower than that of the new generator. Therefore, it was clearly confirmed that the efficiency of the BL-WFSG was decreased because of increasing core losses in the rotor and stator core and the armature and field copper losses with aging. As expected in the Introduction, it was identified that the factor of increasing the field current of the BL-WFSG with aging was the decrease in efficiency due to the increased core loss with aging. This is because the AVR and exciter combination system, which automatically adjusts the magnitude of the field current to constant the output power of the generator, increased the field current to compensate for decreased output power in the same input power.

7. Conclusions

This paper analyzed the material deformation of electrical steel with aging as well as its effects on the electromagnetic, thermal, and efficiency characteristics of the BL-WFSG through the proposed analysis process as shown in Figure 2. To confirm the material deformation due to the aging of the rotor and stator core applied to the BL-WFSG, magnetic property tests were performed on the core sheets extracted from the old and new generators. Through this, the authors verified that the B-H characteristic of the core was rather improved, but the core loss characteristic significantly deteriorated with aging. Based on the magnetic property test results, the electromagnetic field analysis was performed on the old and new generator in order to confirm the effects of material deformation with aging on the electromagnetic characteristics of the BL-WFSG. Through this, it was confirmed that the core loss of the old generator was approximately 179% greater than that of the new generator under the same load condition. It means that the electromagnetic characteristic of the BL-WFSG deteriorated due to material deformation of the core with aging. After that, in order to confirm the effects of material deformation with aging on the thermal characteristics of the BL-WFSG, thermal analysis was performed on the old and new generators using the losses calculated through electromagnetic field analyses as the heat sources. It was confirmed that the temperatures of the armature and field winding of the old generator were higher than that of the new generator. It means that the thermal characteristic of the BL-WFSG deteriorated due to material deformation of the core with aging. Finally, efficiency analyses were performed through additional electromagnetic analysis considering the thermal analysis results. It was confirmed that the efficiency of the old generator was approximately 3.6% lower than that of the new generator. It means that the efficiency characteristic of the BL-WFSG deteriorated due to material deformation of the core with aging. Through this, it was also identified that the factor of increasing the field current of the BL-WFSG with aging was the decrease in efficiency due to the increased core loss with aging.

Author Contributions: Conceptualization, J.-B.K. and J.-Y.L.; methodology, J.-B.K., J.-Y.L. and J.-H.L.; software, J.-B.K. and T.N.; validation, J.-B.K. and J.-Y.L.; formal analysis, J.-B.K.; investigation, J.-B.K. and J.-Y.L.; resources, J.-Y.L.; data curation, J.-B.K., J.-Y.L., T.N. and H.-J.K.; writing—original draft preparation, J.-B.K., H.-J.K. and J.-Y.L.; writing—review and editing, J.-B.K. and J.-Y.L.; visualization, J.-B.K. and T.N.; supervision, J.-Y.L.; project administration, J.-Y.L.; funding acquisition, J.-Y.L. All authors have read and agreed to the published version of the manuscript.

Funding: This research was funded by the KERI Primary research program of MSIT/NST (No. 23A01050).

Data Availability Statement: Not applicable.

Acknowledgments: This research was supported by the Korea Electrotechnology Research Institute (KERI) primary research program through the National Research Council of Science and Technology (NST) funded by the Ministry of Science and ICT (MSIT) (No. 23A01050).

Conflicts of Interest: The authors declare no conflict of interest.

References

1. Nøland, J.K.; Nuzzo, S.; Tessarolo, A.; Alves, E.F. Excitation system technologies for wound-field synchronous machines: Survey of solutions and evolving trends. *IEEE Access* **2019**, *7*, 109699–109718. [CrossRef]
2. Devito, G.; Nuzzo, S.; Barater, D.; Franceschini, G. A Simplified Analytical Approach for Hybrid Exciters of Wound-Field Generators. *IEEE Trans. Transp. Electrif.* **2022**, *8*, 4303–4312. [CrossRef]
3. Wang, Y.; Nuzzo, S.; Zhang, H.; Zhao, W.; Gerada, C.; Galea, M. Challenges and Opportunities for Wound Field Synchronous Generators in Future More Electric Aircraft. *IEEE Trans. Transp. Electrif.* **2020**, *6*, 1466–1477. [CrossRef]
4. Zhang, Z.; Li, W.; Shi, L.; Ma, J.; Yin, Z. A Rotor Position Signal-Free Based Field Current Estimation Method for Brushless Synchronous Starter/Generator. *IEEE Access* **2022**, *10*, 124408–124419. [CrossRef]
5. Nuzzo, S.; Galea, M.; Gerada, C.; Brown, N. Analysis, Modeling, and Design Considerations for the Excitation Systems of Synchronous Generators. *IEEE Trans. Ind. Electron.* **2018**, *65*, 2996–3007. [CrossRef]
6. Nuzzo, S.; Bolognesi, P.; Decuzzi, G.; Giangrande, P.; Galea, M. A Consequent-Pole Hybrid Exciter for Synchronous Generators. *IEEE Trans. Energy Convers.* **2021**, *36*, 368–379. [CrossRef]
7. Ouadah, M.; Toouhami, O.; Ibtiouen, R.; Khorchef, M.; Allou, D. Corrosion effects on the magnetic behavior of magnetic circuit of an induction machine. *Prog. Electromagn. Res. M* **2018**, *68*, 79–87. [CrossRef]
8. Negri, G.M.; Sadowski, N.; Batistela, N.J.; Leite, J.V.; Bastos, J.P. Magnetic aging effect losses on electrical steels. *IEEE Transac. Magn.* **2016**, *52*, 1–4. [CrossRef]
9. de Campos, M.F.; Emura, M.; Landgraf, F.J. Consequences of magnetic aging for iron losses in electrical steels. *J. Magn. Magn. Mater.* **2006**, *304*, e593–e595. [CrossRef]
10. Houguang, C.; Longfei, L.; Lei, L.; Fei, Z.; Sirui, Z.; Libing, Z.; Zhaoguang, D.; Jintao, W. Study on electromagnetic characteristics of silicon steel sheet and transformer vibration under different tension/compression stress. In Proceedings of the 2022 the 15th International Conference on Computer and Electrical Engineering (ICCEE 2022), Journal of Physics: Conference Series, Shenzhen, China, 24–26 June 2022.
11. Perevertov, O.; Thielsch, J.; Schäfer, R. Effect of applied tensile stress on the hysteresis curve and magnetic domain structure of grain-oriented transverse Fe-3%Si steel. *J. Magn. Magn. Mater.* **2015**, *385*, 358–367. [CrossRef]
12. Perevertov, O.; Schäfer, R. Influence of applied tensile stress on the hysteresis curve and magnetic domain structure of grain-oriented Fe–3%Si steel. *J. Phys. D Appl. Phys.* **2014**, *47*, 185001. [CrossRef]
13. Luu, P.T.; Lee, J.Y.; Lee, J.H.; Park, J.W. Electromagnetic and thermal analysis of permanent magnet synchronous motors for cooperative robot applications. *IEEE Trans. Magn.* **2016**, *52*, 1–4. [CrossRef]

14. Cao, L.; Fan, X.; Li, D.; Kong, W.; Qu, R.; Liu, Z. Improved LPTN-Based Online Temperature Prediction of Permanent Magnet Machines by Global Parameter Identification. *IEEE Trans. Ind. Electron.* **2023**, *70*, 8830–8841. [CrossRef]
15. Boglietti, A.; Cavagnino, A.; Staton, D.; Shanel, M.; Mueller, M.; Mejuto, C. Evolution and Modern Approaches for Thermal Analysis of Electrical Machines. *IEEE Trans. Ind. Electron.* **2009**, *56*, 871–882. [CrossRef]
16. Gai, Y.; Kimiabeigi, M.; Chong, Y.C.; Widmer, J.D.; Deng, X.; Popescu, M.; Goss, J.; Staton, D.A.; Steven, A. Cooling of automotive traction motors: Schemes, examples, and computation methods. *IEEE Trans. Ind. Electron.* **2019**, *66*, 1681–1692. [CrossRef]
17. Staton, D.A.; Cavagnino, A. Convection Heat Transfer and Flow Calculations Suitable for Electric Machines Thermal Models. *IEEE Trans. Ind. Electron.* **2008**, *55*, 3509–3516. [CrossRef]
18. Tran., V.K.; Paul, S.; Lee, J.W.; Choi, J.H.; Han, P.W.; Chun, Y.D. System-level consideration and multiphysics design of propulsion motor for fully electrified battery powered car ferry propulsion system. *Electronics* **2023**, *12*, 1491. [CrossRef]